Conference Proceedings

EuroSun 2014
Aix-les-Bains (France), 16 – 19 September 2014

THERMOCHEMICAL SEASONAL STORAGE DEMONSTRATOR FOR A SINGLE-FAMILY HOUSE: DESIGN

Joël Wyttenbach[1], Gwennyn Tanguy[1], Louis Stephan[1]

[1]Univ. Grenoble Alpes, INES, F-73375 Le Bourget du Lac, France

CEA, LITEN, Department of Solar Technologies, F-73375 Le Bourget du Lac, France

Abstract

A seasonal storage demonstration unit coupled with an experimental single family house is being built as part of a solar test platform. It is designed to cover a large fraction of the winter heat load of the house by means of the solar energy collected during summer period.

The core technology consists of an open-cycle thermochemical reactor with strontium bromide as reactant and operated with moist air, acting also as a heat carrier for the space heating system of the house.

The installation includes a solar field, a storage tank, a reactor and a heat-management circuitry conceived with a high degree of flexibility to allow testing different operation modes. This article presents how the system was designed and optimized to reach the best performance both in terms of energy efficiency and compactness.

Keywords: seasonal heat storage, thermochemical storage, moist air, strontium bromide, solar, reactor design.

1. Introduction

Space heating and domestic hot water account for most of the 40.8% households and service final energy consumption in Europe (European commision, 2012, p. 117). Thermal solar panel offer high energy conversion efficiency but without an efficient long term storage system, seasonal time lag reduces solar fraction for heating application. Thermochemical technology offers several major assets such as highest energy density and no systematic energy losses over time. For those reasons, we decided to use it as the core of a seasonal heat storage for an experimental single family house with emulated occupancy behavior (sensible and latent loads). This full scale entire process is a world premiere as is to be launched in 2014 for a two years field test.

2. Thermochemical technology

The thermochemical salt has two stable levels of hydration, so that endothermic dehydration can take place with abundant solar heat, while exothermic hydration is possible when heating is needed.

Those two reactions involve mass transfer of water vapor between thermochemical salt and its environment. Due to working temperatures adapted to space heating and solar collectors, pure water vapor is not available at or above atmospheric pressure. Therefore, the system works either with pure water vapor at a lower pressure, or with a gas mixture including water vapor like moist air.

In any case, the required storage volume depends on its density and on energy needs, which means at least several cubic meters for our single family house. When working with pure water vapor at low pressure, solid reactant material and water have to be stored in vacuum proof containers. In addition, water has to remain in

© 2015. The Authors. Published by International Solar Energy Society
Selection and/or peer review under responsibility of EuroSun2014 Scientific Committee
doi:10.18086/eurosun.2014.10.21 Available at http://proceedings.ises.org

a closed loop circuit in order to limit auxiliary power. Therefore, a specific heat exchanger is required for collecting heat produced or absorbed by the process.

On the other hand, when working with moist air system under atmospheric pressure, there is no need for water storage since water vapor freely available in the air can be used as the second reactant (Michel, et al., 2014) (Bertsch, et al., 2014) Moist air flowing through the thermochemical salt bed porous medium also allows efficient convective heat transfers without the use of any heat exchanger (Ding & Riffat, 2012). For those reasons and because large low pressure vessels are much more complex and expansive to build than atmospheric ones, we chose to build an open loop moist air thermochemical system, as shown in Fig. 1.

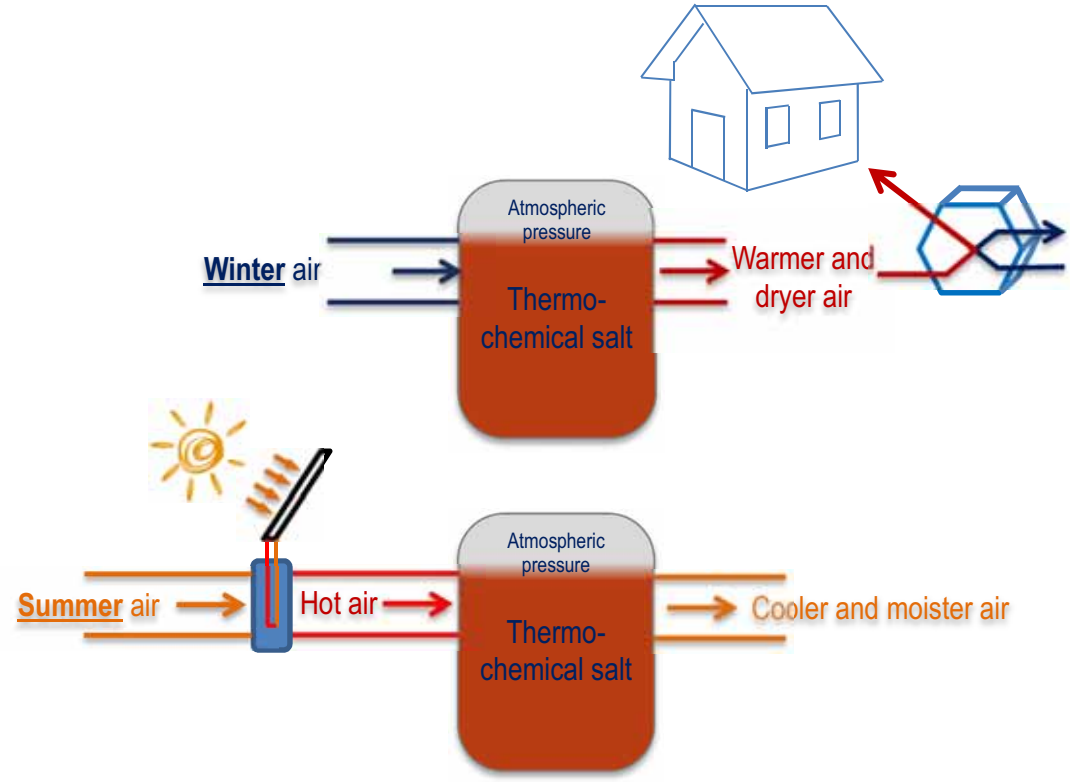

Fig. 1 Thermochemical open loop system, winter and summer circuits

3. Storage size

The required hydrated salt storage size for an entire heating season depends mainly on house heat demand but is also affected by other factors: on one hand, direct solar heating is possible during mid-seasons, but on the other hand, additional heat has to be provided during the days when there is not enough water vapor available in the outside air.

Therefore, for a proper dimensioning of the storage, a dynamic simulation was performed taking into account the complete system. The numerical model includes solar system, thermochemical storage, ventilation, building and duct network. Detailed results of this study are presented in a separate paper, and we focus here on the final strontium bromide hexahydrate storage mass for the tested experimental house: 6000kg. This represents 1580kWh and allows reaching an 84% space heating solar fraction.

4. Reactor typology

The thermochemical solid-gas reaction used for this storage system involves strontium bromide salt and water vapor, as shown in the following equation:

$$SrBr_2.1H_2O + 5(H_2O) \rightleftharpoons SrBr_2.6H_2O + 5\Delta Hr \quad \text{(eq. 1)}$$

Where :

ΔHr	reaction enthalpy	J/mol

Several setups can be found in the literature (Michel, 2012), where reactor and storage are integrated or separated, some of them working under vacuum conditions and others working at atmospheric pressure (Marias, et al., 2014). The fixed bed system under atmospheric pressure was selected for its minimal amount of moving parts and its overall lower technological level. With this technology, moist air flows through bulk salt crystals as it would flow through any porous medium, allowing a good enough residence time between the two reagents. In the same time, this type of circulation means that pressure drop has to be properly assessed when defining system architecture and reactor design, as well as several additional parameters:

- Total solid reactant mass to be stored
- Floor space available for the entire storage
- Maximum floor space and mass per reactor, for transportation and commissioning issues
- Thermal inertia at startup
- Compactness
- Internal air flow repartition
- Internal and external insulation
- Output power correlation to space heating and solar regeneration

After analyzing the above constraints, the best compromise was to have 5 reactors, each with a footprint of 1,5m² and containing 1200kg of hydrated salt. However, splitting the stock into 5 units induces the need for a specific air distribution system able to adapt to different operational modes as described in the following section.

5. Air distribution for a multiple units storage

The system's thermal output power is not constant over seasons, which means that it can use either one or several reactors at a time and operate in parallel or in series. During summertime, a parallel circuit allows solar panel's high thermal power to be absorbed by the storage system, whose individual reactors work at a significantly lower power rate. Besides, as output power of a single reactor decreases with the reaction progress, in wintertime and when reaction is almost complete, the air temperature exiting the reactor falls below the minimum acceptable value for the heating process. At this stage, it is possible to switch to next available reactor, but the first reactor would not be totally discharged. Therefore, a better control strategy would rather temporarily assemble reactors 1 and 2 in series so that reactor 1 can be totally discharged without affecting system's output temperature.

A specific ducting layout was developed to realize all those different circuits with a minimum amount of parts, as shown in Fig. 2. There are 3 dampers and 2 actuators per reactor allowing circuits in series, parallel or with a single reactor. As a result, thermal inertia is reduced, output power variations are possible through dynamic air flow allocation, and only a very small amount of salt remains unused.

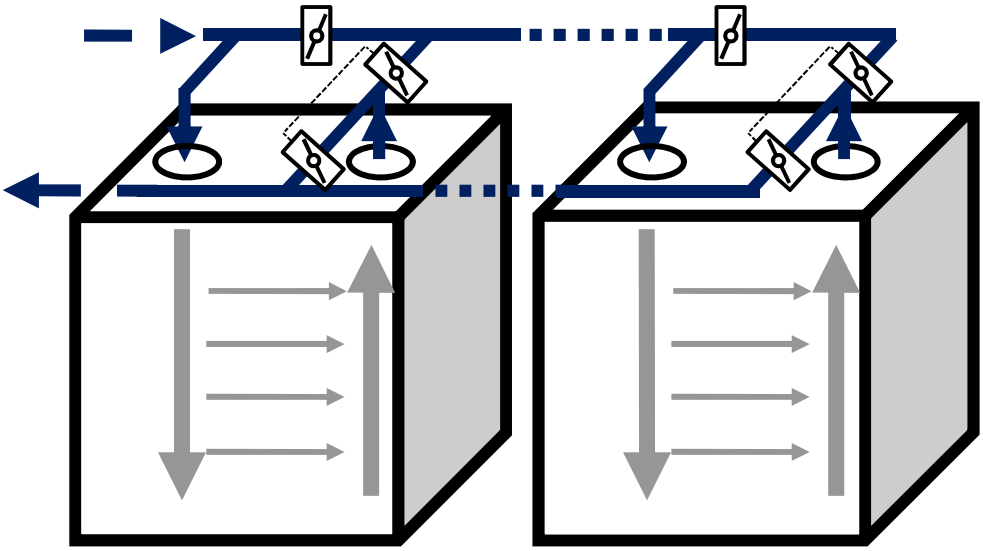

Fig. 2 Reactor with specific air distribution system

6. Reactor Design : pressure drop

Reactor's internal design is highly influenced by pressure drop issues, especially for moist air fixed bed systems. When the salt bed is not reacting, it can be considered as a porous medium that generates a pressure drop as a linear function of air speed. However, there is no simple relation between medium parameters and fixed bed's height. In addition, hydration and dehydration reactions induce geometric changes, thus modifying medium parameters. For those reasons, a number of tests were performed on different fixed bed geometries so that fine interpolations of permeability and porosity can be made in both opposite states, in order to find the best dimensions of the fixed bed, as shown in figure Fig. 3.

Knowing geometric parameters and air flow conditions for a fixed bed reactor, two equations can be written involving pressure drop, permeability and porosity. Following equations come from Darcy's law for fluid flow through a porous medium and from porosity definition.

$$\Delta P = e_s \cdot \frac{Q}{n \cdot S} \frac{\mu}{k} \qquad \text{(eq. 2)}$$

$$e_s = \frac{m_h}{n \cdot (1-\varepsilon) \cdot \rho_h \cdot S} \qquad \text{(eq. 3)}$$

Where:	ΔP	Pressure drop	Pa
	Q	Volume air flow rate	m^3/h
	μ	Air dynamic viscosity	Pa.s
	n	Number of storey	[-]
	S	Fixed bed horizontal surface	m^2
	k	Permeability	m^{-3}
	m_h	Hydrated salt mass in one reactor	kg
	ε	Fixed bed porosity	[-]
	ρ_h	Hydrated salt density	kg/m^3
	p	spline polynomials degree	[-]

Fixed bed permeability and porosity depend on surface density and hydration level. Multi cycle tests performed with SrBr2 hexahydrate show that fixed bed's geometry is not reversible. Therefore, the amount of cycles has to be taken into account for permeability and porosity correlations. However, we did only have upscale experimental available data for three cycles of hydration/dehydration.

Surface density of a storey : $\frac{m_h}{n \cdot S}$.

Permeability per fixed bed thickness is correlated as a spline interpolation of surface density, according to equation (eq. 4) for each interval

$$\left(\frac{k}{e_s}\right)_{h,k} = \sum_{i=0}^{p} a_{i,k} \cdot \left(\frac{m_h}{n.S}\right)^i \qquad \text{(eq. 4)}$$

Similarly, porosity is correlated as a spline interpolation of surface density, according to following equation for each interval

$$\varepsilon_{h,k} = \sum_{i=0}^{p} b_{i,k} \cdot \left(\frac{m_h}{n.S}\right)^i \qquad \text{(eq. 5)}$$

Where :

Subscript h stands for hydrated state

a_i, b_i are polynomial coefficients

k is the interval index

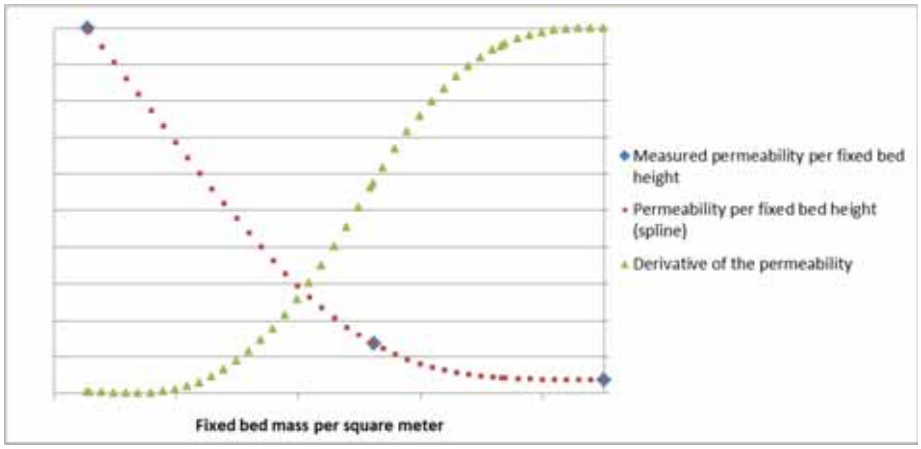

Fig. 3: Permeability spline interpolation as a function of hydrated fixed bed surface density

Similar correlations are set for dehydrated state. In both cases, spline polynomial coefficients are calculated from a set of experimental values as shown in figure Fig. 3. Due to the important upscale factor between laboratory experimentation and this project's reactor size, the first reactor was built using the few test data available at that time. Then, this first reactor was tested, and results were added to available experimental data for further spline interpolation that helped us better optimize the design of the other four reactors.

The reactor's pressure drop influences the fan electrical consumption; therefore we evaluated the maximum allowable value from the target coefficient of performance. The result was a maximum pressure drop of 336 Pa for a given flow rate of 300 m^3/h.

In this case, the maximum pressure drop for a 300 m^3/h flow rate was set at 336 Pa.

Using (eq. 2) to (eq. 5), it is then possible to define the amount of internal parallel

channels needed to reach this maximum pressure drop. In this project, the first reactor features 5 channels (Fig. 6); while the 4 others feature 6 parallel channels. This adaptation results from the test data of the first reactor as cited above.

7. Reactor design : air flow repartition and compactness

As it was shown in the previous section, a reactor is made of five or six parallel channels. In order to reach better reaction performances, air flow through the channels must meet the following criteria:

- Air flow rates running through each channel have to be similar
- Air flowing through the fixed bed has to be evenly distributed over the section plane

In the proposed reactor, the pressure drop induced by the fixed bed predominates the one generated by the surrounding ducts. A CFD analysis was performed in order to assess the issue of air distribution and to validate the final design before manufacturing.

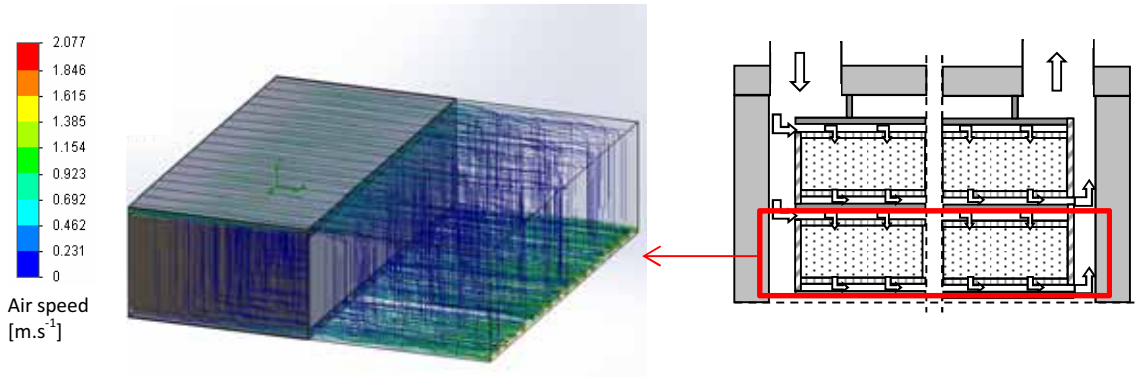

Fig. 4: Streamlines for a partial section of one channel

Fig. 4 shows:

- Gradual air speed decrease in the upper distributor
- Gradual increase in the lower collector
- Generally low speed flow through the porous medium
- No dead zone in the porous medium
- Maximum speed around 2 $m.s^{-1}$

Surface flow homogeneity is assessed by measuring flow rate through virtual surfaces in the simulation model. The results showed that relative deviations stay below 2%.

The whole reactor was also simulated, with a total of 3.6 million CFD cells, as shown in figure 5.

The porous medium model used for this simulation represents the salt bed in its dehydrated state, which is the less favorable for air distribution. Nonetheless, results showed similar flow rates in each channel, with fairly small duct size. This means that we reached a good compromise between air distribution quality and energy density.

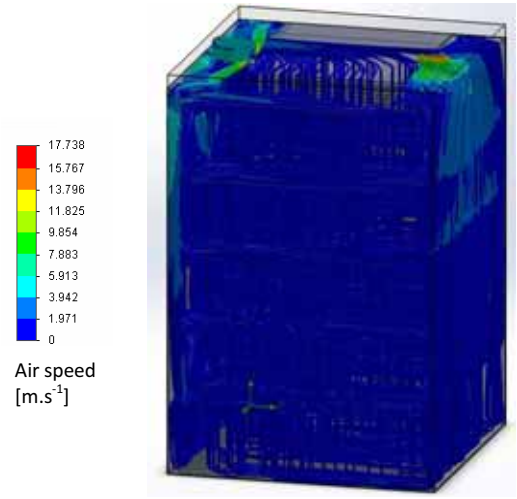

Fig. 5: Whole reactor with streamlines

Fig. 6 shows from left to right:

- One reactor storey with its salt bed and side ducts, also called channel in the CFD simulations
- One whole reactor made of 5 storeys assembled on top of each other
- The experimental house with its storage extension hosting 5 reactors

Fig. 6: Left to right : Salt fixed bed – 5 fixed beds assembled in one reactor – experimental house with its storage extension

8. Energy density discussion

With a density of 2385 kg.m^{-3} and a molar mass of 0,35543 kg.mol^{-1}, the ideal energy density of strontium bromide in its raw and compact version is 628 kWh.m^{-3}. However, for air to flow through the bed, salt should have a minimum degree of porosity, which yields to a significantly lower energy density. Besides, the reactor contains substantial dead volumes represented for example by the heat and mass transfer ducts and by the clearance that must be reserved between the storeys to allow for salt bed volume variations with reaction progress. These dead zones have also a direct impact on the overall reactor density as it is shown in Fig. 7.

Finally, though thermochemical potential remains constant over time, heat losses occur during charging and discharging since both reactions happen at higher temperature than ambience. Therefore, a proper insulation has to be provided to improve the system performance and here again we contribute to another energy density reduction, which is now around 127 kWh.m^{-3}.

During heating season, storage can be partially regenerated, typically during a clear mid-season day. This maneuver increases energy density since the stock is used more than once during the year. Numerical simulations of the global system helped evaluate the annual use rate and its impact on the final energy density (Fig. 7).

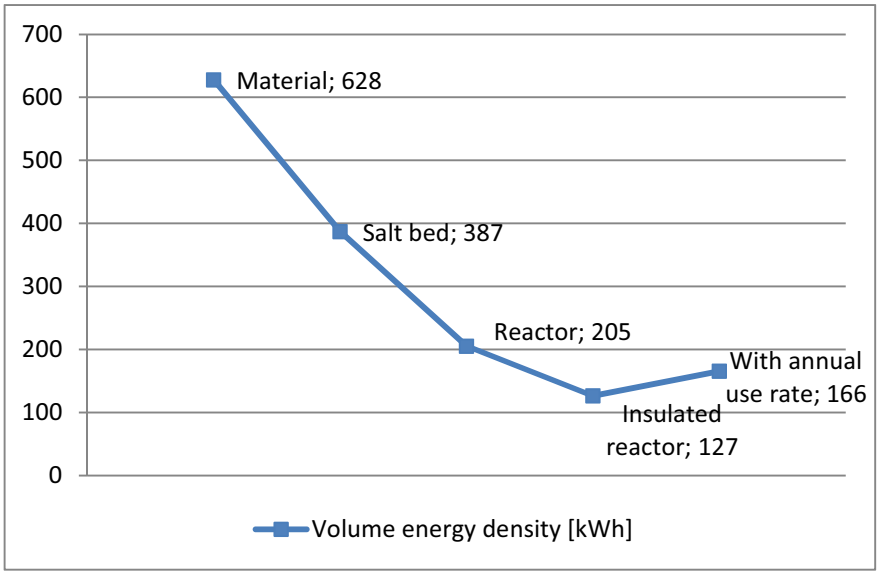

Fig. 7 Volume energy density

To conclude, reactor's energy density is almost 3.8 times lower than that of the raw material. Even though, it is still higher than other storage technologies when considering final product rather than materials. This also shows that there is still a great potential for improving thermochemical reactor energy density by working on its implementation.

9. Conclusion

A first full scale thermochemical seasonal storage demonstrator was built and connected to an experimental house. The expected solar fraction for space heating is up to a record 80%. Reactor design has been optimized to enhance global performance and compactness. CFD simulations helped reducing internal duct sizes while maintaining good flow distribution in each reactor storey. In addition, a specific inter-reactor ducting network was developed to allow heating power modulation and material use-rate optimization. All those improvements made possible to build a heat storage system of 1580 kWh that fits in 12.5 m^3, which is a great performance for a final product compared to other technologies. However, thermochemical material's exceptional built-in energy density shows that further works on implementation techniques can still lead to significant system compactness improvements.

10. References

Bertsch, F. et al., 2014. Comparison of the thermal performance of a solar heating system with open and closed solid sorption storage. *Energy Procedia,* Volume 48, pp. 280-289.

Ding, Y. & Riffat, S. B., 2012. Thermochemical energy storage technologies for building applications: a state-of-the-art review. *International Journal of Low-Carbon Technologies*.

European commision, 2012. *Statistical pocketbook*. s.l.:s.n.

Marias, F., Neveu, P., Tanguy, G. & Papillon, P., 2014. Thermodynamic analysis and experimental study of solid/gas reactor operating in open mode. *Energy*.

Michel, B., 2012. Procédé thermochimique pour le stockage intersaisonnier de l'énergie solaire : modélisation multi-échelles et expérimentation d'un prototype sous air humide http://tel.archives-ouvertes.fr/docs/00/81/88/38/PDF/ThA_se_MICHEL_Benoit.pdf.

Michel, B., Neveu, P. & Mazet, N., 2014. Comparison of closed and open thermochemical processes, for long-term thermal energy storage applications. *Energy,* Volume 72, pp. 702-716.